



## Theory of relativistic radiation reflection from plasmas

Downloaded from: <https://research.chalmers.se>, 2024-03-13 10:26 UTC

Citation for the original published paper (version of record):

Gonoskov, A. (2018). Theory of relativistic radiation reflection from plasmas. *Physics of Plasmas*, 25(1). <http://dx.doi.org/10.1063/1.5000785>

N.B. When citing this work, cite the original published paper.

# Theory of relativistic radiation reflection from plasmas

Arkady Gonoskov<sup>1,2,3</sup>

<sup>1</sup>Department of Physics, Chalmers University of Technology, SE-41296 Gothenburg, Sweden

<sup>2</sup>Institute of Applied Physics, RAS, Nizhny Novgorod 603950, Russia

<sup>3</sup>Lobachevsky State University of Nizhny Novgorod, Nizhny Novgorod 603950, Russia

(Received 18 August 2017; accepted 21 November 2017; published online 4 January 2018)

We consider the reflection of relativistically strong radiation from plasma and identify the physical origin of the electrons' tendency to form a thin sheet, which maintains its localisation throughout its motion. Thereby, we justify the principle of *relativistic electronic spring* (RES) proposed in [Gonoskov *et al.*, Phys. Rev. E **84**, 046403 (2011)]. Using the RES principle, we derive a closed set of differential equations that describe the reflection of radiation with arbitrary variation of polarization and intensity from plasma with an arbitrary density profile for an arbitrary angle of incidence. We confirm with *ab initio* PIC simulations that the developed theory accurately describes laser-plasma interactions in the regime where the reflection of relativistically strong radiation is accompanied by significant, repeated relocation of plasma electrons. In particular, the theory can be applied for the studies of plasma heating and coherent and incoherent emissions in the RES regime of high-intensity laser-plasma interaction. © 2018 Author(s). All article content, except where otherwise noted, is licensed under a Creative Commons Attribution (CC BY) license (<http://creativecommons.org/licenses/by/4.0/>). <https://doi.org/10.1063/1.5000785>

## I. INTRODUCTION

The reflection of electromagnetic radiation from a plasma with overcritical density originates from the induced self-consistent dynamics of electrons at the plasma interface. If the radiation is intense enough to make the electrons' motion relativistic, the radiation pressure causes an inward relocation of electrons and enables a large variety of highly nonlinear reflection scenarios. These span between the cases of ideal reflection (the limit of highly overdense plasma with steep distribution) and relativistic self-induced transparency. Such relativistic intensities can be achieved with high-intensity optical laser pulses, while overdense plasma with various scales of density transition at the interface is naturally formed by the ionization, heating, and thermal expansion of solids exposed to pre-pulse light. The prospects of using laser-solid interactions for various applications, ranging from high-harmonic generation to plasma heating, has stimulated theoretical and experimental studies of the non-linear reflection process.<sup>1–18</sup>

The most general theoretical description of the reflection process is given by the kinetic approach. Although this description is very useful for numerical studies, the high degree of nonlinearity largely precludes direct theoretical analysis based on the kinetic equations. A notable exception is the case of normal incidence of circularly polarized radiation. In this case, the balance between the radiation pressure and the Coulomb attraction to the ions leads to quasi-stationary plasma distributions. These distributions can be obtained analytically in a hydrodynamical approximation.<sup>19,20</sup> However, in other cases, the radiation pressure oscillates in time and gives rise to complex plasma dynamics. Some theoretical analysis can be performed in the limit of high density using the cold fluid approximation.<sup>21–23</sup> However, in the general case, oscillation of the radiation

pressure leads to the formation of many streams in plasmas invalidating the hydrodynamical approximation.

An alternative approach is to develop a simple artificial system, the behaviour of which mimics plasma dynamics in certain aspects. The description in this case can be driven by phenomenological, rather than *ab initio*, principles. If the plasma has a sharp boundary with a steep rise of density to a sufficiently high value, the incident radiation penetrates to a negligible depth, and the deviation from ideal reflection can be modelled using the principle of *relativistic oscillating mirror* (ROM).<sup>24–26</sup> This principle states that the ideal reflection happens at some oscillating point, where the incoming and outgoing electromagnetic fluxes are equal to each other (Leontovich boundary conditions<sup>27</sup>). Theoretical analysis based on the ROM principle provides insights into various aspects of interactions, such as polarization selection rules<sup>5,25,28</sup> and high-harmonic generation properties.<sup>29,30</sup>

However, the assumed-to-be instantaneous redirection of the incident electromagnetic flux implies that energy is not accumulated even for a fraction of the radiation cycle when the electrons are relocated by radiation relative to the ions. Thus, the ROM model cannot encompass effects due to significant electron displacement, which happens when the intensity is not too low and/or the density is not too high. Indeed, the boundary conditions in the ROM model explicitly imply that the amplitude of the reflected radiation can never exceed that of incident radiation. However, for certain parameters, the electron displacement leads to the accumulation of up to 60% of the energy of each radiation cycle, followed by the release of that energy in the form of a short burst with more than a hundred times higher intensity.<sup>31</sup> A principle that accounts for such energy redistribution and describes this and other highly nonlinear interaction

scenarios in this regime was proposed in Ref. 31 and is known as the *relativistic electronic spring* (RES). The RES model provides a direct description of the plasma and electromagnetic field dynamics over a large range of intensities and densities, when the reflection of relativistically strong radiation is accompanied by significant, repeated relocation of plasma electrons. This regime can thus be referred to as the RES regime of laser-plasma interaction. Due to the high degree of energy coupling, the RES regime provides prominent opportunities for plasma heating, as well as for incoherent<sup>32,33</sup> and coherent synchrotron emission (CSE).<sup>34</sup> Instead of the Doppler effect caused by quick phase leaps in the ROM regime or triggered internal plasma oscillations in the regime of coherent wake emission (CWE),<sup>1</sup> the mechanism of high-harmonic generation in the RES regime is a rapid re-emission of the accumulated energy by a thin electron sheet that naturally forms due to relativistic effects.

Recent studies have shown that the RES regime is efficient in converting the energy of incident radiation into coherent XUV bursts with short duration, high intensity<sup>35–37</sup> and controllable ellipticity,<sup>38</sup> as well as for producing incoherent X-ray and gamma radiation.<sup>32,33</sup>

In this paper, we reveal the physical origins of the RES principle and elaborate further on the theory based on this principle. We provide general equations that are applicable for the arbitrary incidence angle, the arbitrary density profile and the arbitrary temporal evolution of the field and polarization in the incident radiation. In this way, we demonstrate that the RES model does not just mimic the reflection process, but is a theory that arises from a physically-grounded approximation.

## II. ORIGINS OF THE GOVERNING PRINCIPLES

The primary assumption of the theory is that the plasma eventually halts the propagation of the incident radiation. This generally happens when the frequency range of the incident radiation is below the plasma frequency. If sufficiently high densities are reached at some point inside the plasma, then the radiation propagation is generally halted. Although effects of relativistic self-induced transparency require more detailed analysis, here, we assume that the density grows at the interface to sufficiently high values to prevent the radiation propagation. Under this assumption, we focus on the origins of the RES principle and answer the following questions: Why do the electrons tend to form a thin sheet? Why do the electrons maintain and sometimes even improve their co-locality in space during the motion of the sheet? Does the RES principle provide a self-consistent description of plasma dynamics under certain assumptions?

We consider the problem in the reference frame moving with velocity  $c \sin \theta$  along the plasma surface, where  $c$  is the speed of light and  $\theta$  is the angle of incidence. In this reference frame, the incidence is normal and the plasma streams with a transverse speed of  $c \sin \theta$ . Under the assumption that the spatial scales of transverse variations of radiation and plasma are large in comparison with the wavelength, the problem can be locally considered as one-dimensional. When the incident radiation reaches the plasma, electrons

start to move under the effect of the electromagnetic fields, while the same fields are modified by the induced electron and ion currents as they propagate deeper and deeper. However, the fact that the propagation of radiation is eventually halted means that the inward emission due to these currents must, at some point, provide exact cancellation of the incident radiation. Thus, the incident field cancellation by the induced currents is a general formulation of the radiation reflection. This cancellation requirement is one of the assumptions of the RES theory.

One might expect the electron spatial distribution, which is determined by the self-consistent electromagnetic fields, to be highly complex. However, a remarkable simplification takes place in the case of relativistic motion: the electrons tend to form a single thin sheet that separates the region of uncompensated ions and the unperturbed plasma.

We observed this tendency and its connection with relativistic effects in the consideration of the stationary problem in Ref. 31. However, this does not explain why it occurs in the general dynamical case: although the electrons can naturally pile up into a localized layer at the rising edge of the radiation pressure, one could expect that the opposite process, i.e., spreading, happens, when the radiation pressure decreases and the layer propagates backwards. However, as one can see from Fig. 3(a) in Ref. 31, the layer actually shrinks even further during this process. This gives rise to the generation of short bursts of radiation. In terms of the acting forces and the consequent particle dynamics, this effect can be qualitatively explained as follows.

We divide the motion of the electrons during a single cycle of radiation pressure oscillations into two stages: first, the radiation pushes electrons from left to right; then in the second stage, the formed layer propagates from right to left (towards the initial position of the plasma boundary). During the first stage, at each instance of time, the following statement holds true: the electrons in the left part of the layer experience a stronger force of radiation pressure for a longer time than the electrons in the right part of the layer. If the force causes a relativistic motion of electrons, then this difference quickly results in piling up the electrons.

During the second stage, the mechanism by which the sheet becomes thinner is different (see Fig. 1). To demonstrate the idea we assume that the density of electrons  $n$  is constant across the layer and that the electrons move with roughly the same speed in the transverse direction (the difference cannot be dramatic because their motion approaches the relativistic limit). We use  $x_r$  to denote the distance between a certain point within the layer and the rightmost side of the layer. In this case, from Ampere's law, we can see that with the increase of  $x_r$ , the transverse component of the magnetic field  $B_\perp$  and the related component of the Lorentz force grow linearly

$$B_\perp \sim nx_r. \quad (1)$$

The residual ions induce a longitudinal electric field that causes attraction of the electrons in the layer to the residual ions. The electrons in the layer compensate this, and the compensation is complete at the most right point of the layer

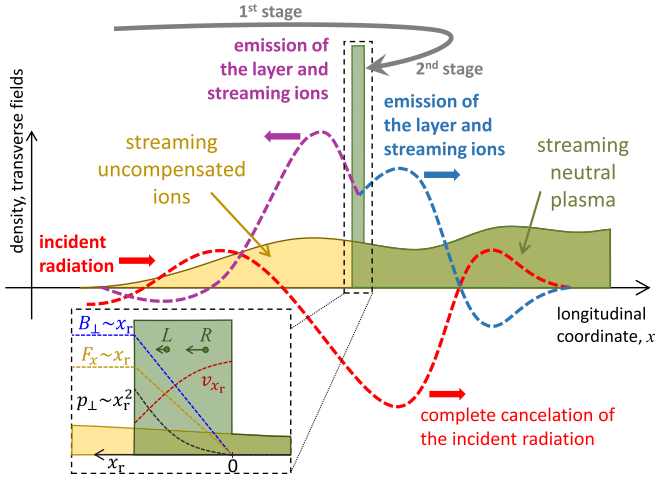


FIG. 1. Schematic representation of the main assumptions and relations.

( $x_r = 0$ ) because of the charge quasineutrality. Under the assumption of the constant density in the layer, the deviation from the complete compensation grows linearly with an increase of  $x_r$ . Thus, the electric component of the Lorentz force also grows linearly with the increase of  $x_r$ . When the attraction to the residual ions starts to dominate over the radiation pressure (determined by  $B_{\perp}$ ), the imbalance also grows linearly with an increase of  $x_r$

$$F_x \sim nx_r. \quad (2)$$

The electrons in the thin layer start to move backward soon after the force of attraction to the residual ions becomes larger than that of the radiation pressure (we will see later that the inertia plays a minor role here). From the conservation of the canonical momentum, we can conclude that the transverse momentum of electrons grows quadratically with  $x_r$  (here, we assume  $p_{\perp} \gg mc$ )

$$p_{\perp} \approx \frac{e}{c} \int_0^{x_r} B_{\perp}(x') dx' \sim nx_r^2, \quad (3)$$

where  $e$  is the electron charge. Thus, the electrons in the left part of the layer have larger values of transverse momentum, and are therefore more “massive” in terms of longitudinal motion due to a relativistic increase of the effective mass. In the highly relativistic case, the effective mass for longitudinal motion grows quadratically with  $x_r$

$$m_{\parallel} = m \sqrt{1 + p_{\perp}^2 / (mc)^2} \sim nx_r^2. \quad (4)$$

As we can see, with an increase of  $x_r$ , the relativistic increase of mass grows quadratically, whereas the longitudinal force grows linearly. This means that the response to the restoring force of the electrons in the left part of the layer is retarded relative to those in the right part. As a result, the electrons in the right part move to the left faster than the electrons in the left part. However, the electrons from the right part can never overrun the electrons from the left part. This is because of the conservation of transverse canonical momentum. Suppose some electron  $L$  had the initial position to the left of some electron  $R$  within the layer and furthermore the electron  $R$  overruns the electron  $L$ , then at some instance of time,

the electrons have the same longitudinal coordinate. At this instance of time, the electrons have exactly the same transverse momentum, because this depends only on the longitudinal coordinate due to the conservation of transverse canonical momentum. However, prior to this instance, the electron  $R$  experienced a strictly weaker longitudinal force and thus gained less longitudinal momentum than the electron  $L$ . Thus, the electron  $R$  has strictly smaller longitudinal velocity than the electron  $L$ . This contradicts the initial supposition that the electron  $R$  overruns the electron  $L$ . The consequence of this is that the electrons in the layer can come closer to each other, but the effect of wave breaking can never happen.

In such a way, we showed that in the case of relativistic motion, the relativistic mass increase due to transverse momentum causes an inversion of longitudinal velocities in the layer, while the conservation of transverse canonical momentum prevents breaking of this inversion. Therefore, the layer tends to shrink during its backward motion. This means that the electrons in the layer tend towards having the same longitudinal velocity. Since their motion is relativistic, and the orientation of the transverse motion is roughly the same (being determined by the magnetic field orientation), the transverse components of the electrons’ velocities are roughly the same for all electrons within the layer. This provides complete self-consistency with the macroscopic assumptions of the RES theory. In the RES theory, we make use of the fact that the emission is determined by the electrons’ velocity but not momentum. Thus, although the electrons in the layer do have different values of momentum, their emission can be described in terms of macroscopic parameters: the layer’s charge and velocity.

The only special point in this respect is the point when the layer moves almost exactly to the left. In this case, the backward emission becomes singularly strong because Eqs. (8) and (9) are divergent at  $\beta_x = -1$ . The actual limit depends on the gamma factor distribution and the thickness of the layer. Determining the actual limit of the layer’s shrinking requires consideration of its microscopic dynamics. The driving conditions for these dynamics can be obtained from its macroscopic dynamics described by RES theory under the assumption of the layer being thin in comparison with its macroscopic motion.

### III. GOVERNING EQUATIONS

Here, we again use the moving reference frame, where the incidence is normal and the problem can be considered as one-dimensional. Although we use this approximation here, the developed approach can be extended to account for various deviations from one-dimensional geometry. We also assume here that ions remain immobile, but their motion can be accounted for, for example, as a slow deviation to the presented consideration. We use an orthogonal coordinate system  $XYZ$  with the  $x$ -axis oriented towards the incidence direction and the  $y$ -axis oriented against the plasma stream.

The RES principle includes three assumptions:<sup>31</sup> (1) at each instance of time, the electrons, pushed by the incident radiation, form a thin layer that separates unperturbed plasma



and the region of uncompensated ions; (2) electrons in the layer may have different gamma factors, but move with a relativistic speed in the same direction; and (3) the motion of electrons together with the flow of uncompensated ions produces emission that cancels the incident radiation behind the thin layer (see Fig. 1). We use these assumptions here to derive a generalized theory of interaction in the RES regime.

According to the RES principle, at each instance of time, the plasma is assumed to consist of three regions: (1) a region  $x < x_s$  that contains only plasma ions but no electrons; (2) a thin sheet of electrons at  $x = x_s$ , where the uncompensated charge of the first region is concentrated; and (3) unperturbed plasma for  $x > x_s$ . The RES principle states that radiation of the electrons in the thin layer and of uncompensated ions provide compensation for the incident radiation

$$E_y(\cos \theta(x_s - ct)) = \frac{2\pi e}{\cos^2 \theta} \int_{-\infty}^{x_s} N(x) dx \left( \sin \theta - \frac{\beta_y}{1 - \beta_x} \right), \quad (5)$$

$$E_z(\cos \theta(x_s - ct)) = \frac{2\pi e}{\cos^2 \theta} \int_{-\infty}^{x_s} N(x) dx \left( -\frac{\beta_z}{1 - \beta_x} \right), \quad (6)$$

where the arbitrary incident radiation is characterized in the laboratory frame through the electric field (in CGS units) in the plane of incidence  $E_y(\eta)$  and in the other transverse direction  $E_z(\eta)$  as functions of coordinate  $\eta$  along the propagation (for the respective components of the magnetic field, this implies  $B_z(\eta) = E_y(\eta)$  and  $B_y(\eta) = -E_z(\eta)$ ); the plasma is characterized by an arbitrary function  $N(\chi)$  of ion density in the laboratory frame as a function of depth  $\chi$ ;  $\beta_x$ ,  $\beta_y$  and  $\beta_z$  are the effective (averaged) components of the electron velocity in the sheet given in the units of the speed of light. If the fields are sufficiently strong to cause a relativistic motion of electrons, the limit  $\beta_x^2 + \beta_y^2 + \beta_z^2 = 1$  can be used to account for relativistic restriction. Note that the relativistic gamma factor does not directly enter the expressions for the layer emission. In some cases, it might be important to consider the finite value of the gamma factor; however, as we understood above, the gamma factor is different for different electrons in the layer. Thus, the above-mentioned relativistic limit provides a natural self-consistent description in a simple form. Using that  $q_s = 2\pi e \int_{-\infty}^{x_s} N(x) dx / \cos^2 \theta$  characterizes the instantaneous total charge of electrons in the layer, we can now write a closed system of differential equations that describe the reflection process

$$\begin{cases} E_y(\cos \theta(x_s - ct)) = q_s \left( \sin \theta - \frac{\beta_y}{1 - \beta_x} \right), \\ E_z(\cos \theta(x_s - ct)) = q_s \left( -\frac{\beta_z}{1 - \beta_x} \right), \\ \beta_x^2 + \beta_y^2 + \beta_z^2 = 1, \\ \frac{dq_s}{dt} = \frac{2\pi e c}{\cos^2 \theta} N(x_s) \beta_x, \\ \frac{dx_s}{dt} = c \beta_x. \end{cases} \quad (7)$$

During the reflection process, the backward emission appears as the component of the radiation of the uncompensated ions and the electrons in the layer in the negative  $x$  direction

$$E_y^b(\cos \theta(x_s + ct)) = q_s \left( \frac{\beta_y}{1 + \beta_x} - \sin \theta \right), \quad (8)$$

$$E_z^b(\cos \theta(x_s + ct)) = q_s \left( \frac{\beta_z}{1 + \beta_x} \right), \quad (9)$$

where the backward radiation is characterized in the laboratory frame through the electric field in the plane of incidence  $E_y^b(\xi)$  and in the other transverse direction  $E_z^b(\xi)$  as functions of coordinate  $\xi$  along the specular direction (for the respective components of the magnetic field, this implies  $B_z^b(\xi) = -E_y^b(\xi)$  and  $B_y^b(\xi) = E_z^b(\xi)$ ).

We can now show that system (7) always provides exactly one solution, and that this solution is physically meaningful. From the first three equations, we can explicitly obtain

$$\beta_x = \frac{R_y^2 + R_z^2 - 1}{R_y^2 + R_z^2 + 1}, \quad (10)$$

where the quantities  $R_y = \beta_y / (1 - \beta_x)$  and  $R_z = \beta_z / (1 - \beta_x)$  are given by

$$R_y = \sin \theta - \frac{E_y(\cos \theta(x_s - ct))}{q_s}, \quad (11)$$

$$R_z = -\frac{E_z(\cos \theta(x_s - ct))}{q_s}. \quad (12)$$

Expression (10) always provides a value within a meaningful range  $-1 < \beta_x < 1$ . Another requirement for the solution to be meaningful occurs under the assumption that the plasma has a certain bound, which we can assume to be at  $x = 0$ , i.e.,  $N(x < 0) = 0$ ,  $N(x > 0) > 0$ . In this case, the solution has a physical meaning only if  $x_s > 0$ . We can show that this is always the case. If the value of  $x_s$  approaches the point  $x = 0$ , the value of  $q_s$  also tends to zero. In this case, according to Eqs. (11) and (12), the value  $R_y^2 + R_z^2$  tends to grow (if  $E_y \neq 0$  or  $E_z \neq 0$ ). This eventually leads to  $\beta_x > 0$  [see Eq. (10)], precluding reaching the point  $x = 0$ . The only exception is the case when both  $E_y = 0$  and  $E_z = 0$ . This can happen when the polarization is strictly linear. In this case, one can consider a linear approximation of the field in the vicinity of the zero point and demonstrate that the linearised equations always give a positive solution for  $\beta_x$ . Thus, passing this special point implies that  $\beta_x$  switches from negative to positive instantly at  $x = 0$ . (This result is expected, since we can always introduce a small deviation from linear polarization to resolve this special point and then consider the limit of the deviation to be infinitely small.)

We have demonstrated that the theory always provides exactly one solution, and this solution is physically meaningful. Then, Eqs. (10)–(12) provide a practical means of computing the solution numerically. Assuming that at the instance of time  $t = 0$ , the incident radiation reaches the

plasma at the point  $x=0$  [i.e.,  $E_y(\eta > 0) = 0$ ,  $E_z(\eta > 0) = 0$ ,  $N(d < 0) = 0$ ], we can write the initial conditions for system (7) in the form

$$x_s(t=0) = 0, \quad (13)$$

$$q_s(t=0) = 0. \quad (14)$$

Equations (10)–(12) coupled with the last two equations of system (7) explicitly determine how  $x_s$  and  $q_s$  evolve, provided that we start from any negligibly small, but non-zero values of  $x_s$  and  $-q_s$  (which is justified by the interest in the solution with a physical meaning). For practical reasons, one can also avoid the aforementioned singular point by introducing a small deviation to the field in the points where  $E_y = 0$  and  $E_z = 0$ . These practically motivated deviations do not affect the results.

The equations of system (7) are self-similar under multiplication of the density and amplitude distributions by the same factor. This means that the developed theory is relativistically self-similar. Note, however, that in the general case, the arbitrary variation of fields and density does not allow defining any certain frequency, amplitude, density and thus the value of relativistic similarity parameter<sup>26</sup>  $S = n/a$ , where  $n$  and  $a$  are the plasma density in units of critical density and the radiation amplitude in relativistic units.

#### IV. COMPARISON WITH NUMERICAL SIMULATIONS

To demonstrate the capabilities of the theory, we present a comparison of the theoretical results with the results of a PIC simulation for a particular interaction scenario. We consider a pulse of radiation incident on a plasma slab with an incidence angle of  $\theta = \pi/7$ . We again consider the problem in the moving reference frame, where the problem is one-dimensional. In this reference frame, the pulse is defined by the field components  $E_y(x-t) = B_z(x-t) = 300 \sin(x-t)$ ,  $E_z(x-t) = -B_y(x-t) = 150 \sin((x-t)7/4)$ , where coordinate  $x$  and time  $t$  are given in the units of  $\lambda/(2\pi)$  and  $\lambda/(2\pi c)$ , respectively, and the field strength is given in relativistic units  $2\pi c^2/(e\lambda)$ ,  $\lambda = (1 \mu\text{m})/\cos\theta$ . The plasma comprises immobile ions and electrons with the density rising linearly from 0 to 500 over  $0 < x < \lambda/3$ , staying fixed over  $\lambda/3 < x < 2\lambda/3$  and falling linearly to 0 over  $2\lambda/3 < x < \lambda$ . Here, the density is given in units of  $n_{\text{cr}}/\cos\theta$ , where  $n_{\text{cr}} = \pi mc^2/(e\lambda)^2$  is the plasma critical density for the wavelength  $\lambda$  in the laboratory frame.

The results of 1D PIC simulation for this problem are shown in Fig. 2 for four instances of time. At the instance  $t=4.4$ , we can clearly see how the incident radiation pushes electrons so that they form a dense layer. At the instance  $t=5.5$ , we can see how this layer shrinks further during its backward motion and how this results in the generation of a singular burst of radiation. At the last instance  $t=15.7$ , we can see the resulting reflected radiation. The result of numerical integration of system (7) is shown with dotted curves in terms of  $E_y(x+t) = -B_z(x+t)$  and  $E_z(x+t) = B_y(x+t)$  calculated via Eqs. (8) and (9). As we can see, the theory describes the entire process well. The most difficult instance for the theory is the instance of the burst generation, when

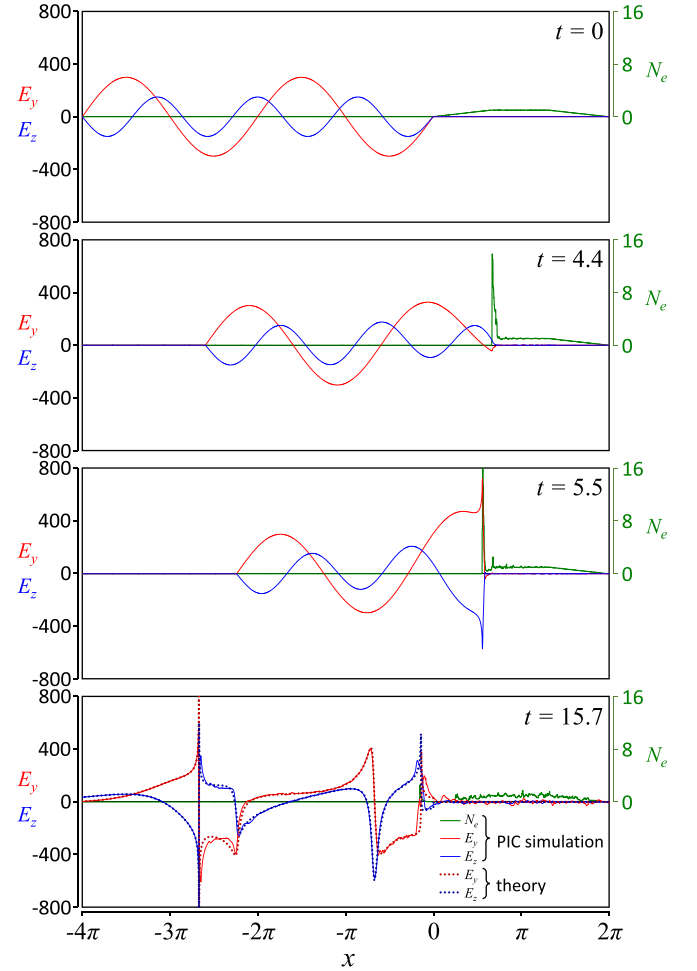


FIG. 2. Comparison of theoretical calculations with the result of PIC simulation for the scenario described in the text. The panels show the electric field  $y$ - and  $z$ -components and the electron density as a function of the longitudinal coordinate in the moving reference frame for four instances of time:  $t=0$  (initial distributions),  $t=4.4$  (radiation pushing electrons that pile up into a layer),  $t=5.5$  (the layer shrinking during backward motion),  $t=15.7$  (the resultant reflected signal that propagates from right to left). The results of numerical integration of the theory equations are shown with dotted curves for  $t=15.7$ .

$\beta_x \approx -1$ . At this point, the theory gives singular results because the gamma factor is assumed to be infinite. The results are not so sensitive to this assumption at other instances of time. The analysis presented above shows that it is not reasonable to consider any particular value of gamma factor, because it is different for different electrons within the layer. This point is of particular interest for the generation of short bursts of radiation and plasma heating because the electron layer undergoes the most extreme bifurcation. To study these problems, one needs to consider micro-dynamics of the electron layer. The presented theory can be very useful for determining the macroscopic conditions for these studies.

As one can see from the picture for  $t=15.7$  after the singular point at  $x \approx -2.6\pi$ , the resultant emission starts to deviate slightly (in a non-systematic but rather random way) from the predictions of the theory at  $x > -2.6\pi$ . However, these deviations quickly decay and the generated signal again follows perfectly the prediction from  $x > -2\pi$ . This indicates that the theory encompasses the essence of the

plasma dynamics, while the particular perturbations decay quickly so that the plasma does not accumulate and “remember” earlier deviations. The parameters of the considered example have been chosen arbitrarily; similar or even better agreement can be seen in other cases for the same level of intensity.

However, the accuracy of description depends on how relativistic the motion is. In the case of a wave with constant frequency  $\omega$ , this can be characterized by a parameter  $a_0$ , which is the wave amplitude in relativistic units  $mc\omega/e$ . The theory is not restricted to any certain frequency of the incident radiation (which can have a broad spectrum) and thus the definition of  $a_0$  is not straightforward in the general case. However, in order to provide a general sense of the theory’s accuracy for different intensities, we present here the results of several relativistically similar problems, defining  $a_0$  using the frequency and the amplitude of the wave that comprises the  $E_y$  component inside the incident pulse. In Fig. 3, we show the results of PIC simulations for  $a_0 = 300$  (as considered above),  $a_0 = 30$  and  $a_0 = 3$ . To maintain relativistic self-similarity, the density and field amplitudes in the last two cases are accordingly multiplied by 0.1 and 0.01, respectively; all other parameters and distributions are the same as before. As one can see from Fig. 3(a), in terms of the field peaks and their position, the theory captures the essence of the plasma dynamics even for moderately relativistic intensities ( $a_0 \sim 3$ ), while the agreement becomes almost perfect for highly relativistic intensities ( $a_0 \sim 300$ ).

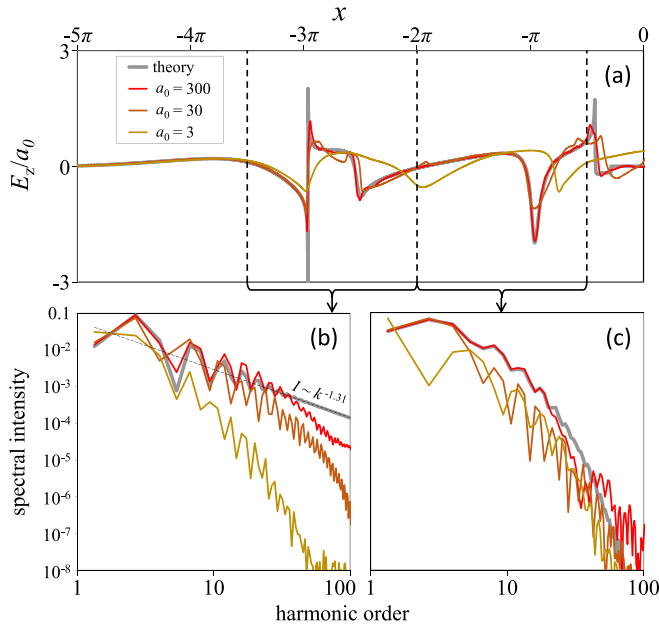


FIG. 3. Comparison of theoretical calculations (grey) with the results of PIC simulations for the set-ups relativistically similar to that in Fig. 2, but with different field amplitudes characterized by  $a_0 = 300$  (red),  $a_0 = 30$  (orange) and  $a_0 = 3$  (yellow) (see the definition of  $a_0$  in the text). The panel (a) shows the electric field  $z$ -component in units of  $a_0$  as a function of coordinate at the instance of time  $t = 16.6$ . The spectrum of this component is shown separately for two windows:  $-3.5\pi < x < -2\pi$  [panel (b)] and  $-2\pi < x < -0.5\pi$  [panel (c)]. (To avoid the artificial high-frequency background, the signals were smoothed to zero at both ends within  $3\pi/32$ .) The black dashed line in panel (b) shows the fitted power law determined for the grey curve.

Therefore, we conclude that the theory correctly and accurately describes the ultra-relativistic limit of plasma dynamics and also provides a guiding description at moderately relativistic intensities. We can see that the singular bursts predicted by the theory appear in the simulations in the calculated form only in the case of sufficiently high intensity, i.e., when the relativistic effects lead to shrinking of the thin layer to a thickness less than the thickness of the radiation burst. For the burst at  $x \approx -\pi$ , the PIC simulation reproduces the calculated form perfectly already for  $a_0 = 300$ , while the peak at  $x \approx -3\pi$  is more singular and thus not reproduced completely even at this intensity. This can also be seen from the spectra presented separately for these peaks in Figs. 3(b) and 3(c): the spectrum obtained from the PIC simulation for  $a_0 = 300$  almost perfectly coincides with the theoretical result for the peak at  $x \approx -\pi$ , whereas for the peak at  $x \approx -3\pi$ , the numerical results start to deviate in the high-frequency region (where the fitted power law is  $I \sim k^{-1.31}$ , with  $I$  being the spectral intensity and  $k$  being the harmonic order). We can also see a clear tendency of the numerical results to fit the theoretical results for larger and larger frequency ranges with the increase of intensity.

This clearly demonstrates that for moderate intensities, the developed theory distinguishes and describes the essential dynamics of plasma and the general form of the reflected radiation, while some properties of the singularly generated bursts, their amplitudes and spectra may depend on the internal properties of the formed thin layer (such as the actual thickness and the distribution of the electron gamma factor). In this respect, by determining macroscopic external conditions for the thin layer, the theory provides an essential basis for determining its microscopic dynamics and the properties of its emission in the vicinity of singularity points.

## V. CONCLUSIONS

In this paper, we have identified the physical origins of the RES principles and demonstrated that these principles emerge from the general tendency of electrons to bunch into a thin sheet due to relativistic effects in radiation-plasma interactions of arbitrary type. Using the RES principles, we developed a theory that is capable of describing radiation-plasma interactions for the arbitrary variation of polarization and intensity in the incident radiation, the arbitrary density profile of irradiated plasma, as well as the arbitrary angle of incidence. The theory can be applied for studies of surface high-harmonic generation and plasma heating with intense lasers. It can also guide theoretical and experimental studies by revealing the dependence of interaction scenarios on the incidence angle, the shape of the plasma density profile, as well as the laser pulse shape, intensity, ellipticity, and carrier-envelope phase.

## ACKNOWLEDGMENTS

The author would like to thank M. Marklund and T. G. Blackburn for useful discussions. The research was supported by the Russian Science Foundation Project No. 16-12-10486, Swedish Research Council Grant Nos. 2013-

4248 and 2016-03329, and the Knut & Alice Wallenberg Foundation.

- <sup>1</sup>F. Quéré, C. Thauray, P. Monot, S. Dobosz, P. Martin, J.-P. Geindre, and P. Audebert, *Phys. Rev. Lett.* **96**, 125004 (2006).
- <sup>2</sup>B. Dromey, M. Zepf, A. Gopal, K. Lancaster, M. S. Wei, K. Krushelnick, M. Tatarakis, N. Vakakis, S. Moustazis, R. Kodama, M. Tampo, C. Stoeckl, R. Clarke, H. Habara, D. Neely, S. Karsch, and P. Norreys, *Nat. Phys.* **2**, 456 (2006).
- <sup>3</sup>C. Thauray, F. Quéré, J.-P. Geindre, A. Levy, T. Ceccotti, P. Monot, M. Bougeard, F. Réau, P. d'Oliveira, P. Audebert, R. Marjoribanks, and P. Martin, *Nat. Phys.* **3**, 424 (2007).
- <sup>4</sup>B. Dromey, D. Adams, R. Hrlein, Y. Nomura, S. Rykovanov, D. Carroll, P. Foster, S. Kar, K. Markey, P. McKenna, D. Neely, M. Geissler, G. Tsakiris, and M. Zepf, *Nat. Phys.* **5**, 146 (2009).
- <sup>5</sup>U. Teubner and P. Gibbon, *Rev. Mod. Phys.* **81**, 445 (2009).
- <sup>6</sup>P. Heissler, R. Hörlein, M. Stafe, J. M. Mikhailova, Y. Nomura, D. Herrmann, R. Tautz, S. G. Rykovanov, I. B. Földes, K. Varjú, F. Tavella, A. Marcinkevicius, F. Krausz, L. Veisz, and G. D. Tsakiris, *Appl. Phys. B* **101**, 511 (2010).
- <sup>7</sup>P. Heissler, R. Hörlein, J. M. Mikhailova, L. Waldecker, P. Tzallas, A. Buck, K. Schmid, C. M. S. Sears, F. Krausz, L. Veisz, M. Zepf, and G. D. Tsakiris, *Phys. Rev. Lett.* **108**, 235003 (2012).
- <sup>8</sup>J. M. Mikhailova, M. V. Fedorov, N. Karpowicz, P. Gibbon, V. T. Platonenko, A. M. Zheltikov, and F. Krausz, *Phys. Rev. Lett.* **109**, 245005 (2012).
- <sup>9</sup>C. Rödel, D. an der Brügge, J. Bierbach, M. Yeung, T. Hahn, B. Dromey, S. Herzer, S. Fuchs, A. G. Pour, E. Eckner, M. Behmke, M. Cerchez, O. Jäckel, D. Hemmers, T. Toncian, M. C. Kaluza, A. Belyanin, G. Pretzler, O. Willi, A. Pukhov, M. Zepf, and G. G. Paulus, *Phys. Rev. Lett.* **109**, 125002 (2012).
- <sup>10</sup>H. Vincenti, S. Monchocé, S. Kahaly, G. Bonnaud, P. Martin, and F. Quéré, *Nat. Commun.* **5**, 3403 (2014).
- <sup>11</sup>C. Riconda, S. Weber, L. Lancia, J.-R. Marquès, G. Mourou, and J. Fuchs, *Plasma Phys. Controlled Fusion* **57**, 014002 (2014).
- <sup>12</sup>G. Fiore, R. Fedeles, and U. de Angelis, *Phys. Plasmas* **21**, 113105 (2014).
- <sup>13</sup>G. Ma, W. Yu, M. Y. Yu, B. Shen, and L. Veisz, *Opt. Express* **24**, 10057 (2016).
- <sup>14</sup>M. R. Edwards and J. M. Mikhailova, *Phys. Rev. A* **93**, 023836 (2016).
- <sup>15</sup>M. R. Edwards and J. M. Mikhailova, *Phys. Rev. Lett.* **117**, 125001 (2016).
- <sup>16</sup>V. V. Strelkov, V. T. Platonenko, A. F. Sterzhantov, and M. Y. Ryabikin, *Phys.-Usp.* **59**, 425 (2016).
- <sup>17</sup>A. Leblanc, A. Denoeud, L. Chopineau, G. Mennerat, P. Martin, and F. Quéré, *Nat. Phys.* **13**, 440 (2017).
- <sup>18</sup>S. Chatziathanasiou, S. Kahaly, E. Skantzakis, G. Sansone, R. Lopez-Martens, S. Haessler, K. Varju, G. Tsakiris, D. Charalambidis, and P. Tzallas, *Photonics* **4**, 26 (2017).
- <sup>19</sup>A. Kim, F. Cattani, D. Anderson, and M. Lisak, *JETP Lett.* **72**, 241 (2000).
- <sup>20</sup>F. Cattani, A. Kim, D. Anderson, and M. Lisak, *Phys. Rev. E* **62**, 1234 (2000).
- <sup>21</sup>J. Sanz, A. Debayle, and K. Mima, *Phys. Rev. E* **85**, 046411 (2012).
- <sup>22</sup>A. Debayle, J. Sanz, L. Gremillet, and K. Mima, *Phys. Plasmas* **20**, 053107 (2013).
- <sup>23</sup>A. Debayle, J. Sanz, and L. Gremillet, *Phys. Rev. E* **92**, 053108 (2015).
- <sup>24</sup>S. V. Bulanov, N. M. Naumova, and F. Pegoraro, *Phys. Plasmas* **1**, 745 (1994).
- <sup>25</sup>R. Lichters, J. MeyerterVehn, and A. Pukhov, *Phys. Plasmas* **3**, 3425 (1996).
- <sup>26</sup>S. Gordienko, A. Pukhov, O. Shorokhov, and T. Baeva, *Phys. Rev. Lett.* **93**, 115002 (2004).
- <sup>27</sup>A. Bourdier, *Phys. Fluids* **26**, 1804 (1983).
- <sup>28</sup>D. von der Linde and K. Rzàzewski, *Appl. Phys. B* **63**, 499 (1996).
- <sup>29</sup>T. Baeva, S. Gordienko, and A. Pukhov, *Phys. Rev. E* **74**, 046404 (2006).
- <sup>30</sup>A. S. Pirozhkov, S. V. Bulanov, T. Z. Esirkepov, M. Mori, A. Sagisaka, and H. Daido, *Phys. Plasmas* **13**, 013107 (2006).
- <sup>31</sup>A. A. Gonoskov, A. V. Korzhimanov, A. V. Kim, M. Marklund, and A. M. Sergeev, *Phys. Rev. E* **84**, 046403 (2011).
- <sup>32</sup>E. N. Nerush, I. Y. Kostyukov, L. Ji, and A. Pukhov, *Phys. Plasmas* **21**, 013109 (2014).
- <sup>33</sup>D. Serebryakov, E. Nerush, and I. Y. Kostyukov, *Phys. Plasmas* **22**, 123119 (2015).
- <sup>34</sup>D. an der Brügge and A. Pukhov, *Phys. Plasmas* **17**, 033110 (2010).
- <sup>35</sup>A. Bashinov, A. Gonoskov, A. Kim, G. Mourou, and A. Sergeev, *Eur. Phys. J.: Spec. Top.* **223**, 1105 (2014).
- <sup>36</sup>J. Fuchs, A. Gonoskov, M. Nakatsutsumi, W. Nazarov, F. Qur, A. Sergeev, and X. Yan, *Eur. Phys. J.: Spec. Top.* **223**, 1169 (2014).
- <sup>37</sup>T. G. Blackburn, A. A. Gonoskov, and M. Marklund, preprint [arXiv:1701.07268](https://arxiv.org/abs/1701.07268) (2017).
- <sup>38</sup>M. Blanco, M. T. Flores-Arias, and A. Gonoskov, preprint [arXiv:1706.04785](https://arxiv.org/abs/1706.04785) (2017).